Article

A Methodology and Experimental Implementation for Industrial Robot Health Assessment via Torque Signature Analysis

Unai Izagirre * [ID]**, Imanol Andonegui, Aritz Egea and Urko Zurutuza** [ID]

Electronics and Computer Science Department, Mondragon Unibertsitatea, 20500 Arrasate, Spain; iandonegui@mondragon.edu (I.A.); aegea@mondragon.edu (A.E.); uzurutuza@mondragon.edu (U.Z.)
* Correspondence: uizagirre@mondragon.edu

check for updates

Abstract: This manuscript focuses on methodological and technological advances in the field of health assessment and predictive maintenance for industrial robots. We propose a non-intrusive methodology for industrial robot joint health assessment. Torque sensor data is used to create a digital signature given a defined trajectory and load combination. The signature of each individual robot is later used to diagnose mechanical deterioration. We prove the robustness and reliability of the methodology in a real industrial use case scenario. Then, an in depth mechanical inspection is carried out in order to identify the root cause of the failure diagnosed in this article. The proposed methodology is useful for medium and long term health assessment for industrial robots working in assembly lines, where years of almost uninterrupted work can cause irreversible damage.

Keywords: PHM; industrial robots; Industry 4.0; predictive maintenance

1. Introduction

In recent decades, research in industrial robots focused mainly on improving manufacturing processes, optimizing trajectories, improving accuracy, etc. However, predictive maintenance and health assessment of robots, has not received as much attention [1,2]. From a maintenance point of view, industrial robots are a complex kinematic chain comprised of several mechanical components that have been extensively studied individually: Motors, speed reducers, gears and bearings just to cite some. Notwithstanding, the union of all these components in a single system and its maintenance as a whole, significantly increases the complexity of failure prediction. In general, health assessment techniques for machinery can be classified in two main groups: physical model-based and data-driven [3]. The former uses deterministic mathematical models to describe the expected behavior of a given system and compares this expected behavior with the real behavior. The latter, analyses data captured with sensors and applies statistical and machine learning methods to detect patterns and predict behavior.

Model-based approaches have been widely used to detect failures in industrial components [4–6]. Unfortunately, it is often difficult to implement an analytical model that accurately describes the behavior of such complex systems. In order to build an analytical model of an industrial robot, there are some approximations and assumptions that have to be made such as constant speeds, temperature of the lubricant, loads, etc. [7]. These necessary approximations distance the model from the real behavior of the system, thus data-driven approaches can be more accurate for industrial robot health assessment [1]. In addition, the expansion of the Industrial Internet of Things (IIoT) and Big Data technology in the era of smart manufacturing [8] is pushing the way towards the implementation of reliable data analysis solutions for predictive maintenance.

Data-based monitoring and IoT solutions are rapidly emerging and transforming the manufacturing industry into an industrial Big Data environment [9]. Several research groups have addressed the issue of monitoring the mechanical condition of machine-tools and industrial robots with data-driven approaches [10–13]. Mourtzis et al. [14] developed a holistic framework for milling and CNC machine tool modelling using the OPC-UA communication standard. They implemented a data acquisition device in order to integrate machine-tools without connectivity in their solution. Vogl et al. [15] proposed a multi-sensor system for machine tool axes monitoring and degradation assessment. A.A. Jaber [2] developed an embedded system for industrial robot condition monitoring using accelerometers at the flange of the robot. He detected a mechanical failure in the gears of the robot joints and emphasized the need for more research in the field of robot predictive maintenance. The drawback of using this approach for robots in a real assembly line is that it is hard to isolate external vibrations from vibration caused by the robot's failure. To overcome this issue, acoustic emission sensors were used in [16] to detect a faulty rolling bearing on a welding robot joint. An important issue to take into account with both accelerometers and acoustic emission sensors, is that they are intrusive in the sense that they have to be attached to the structure of the robot. This can be a drawback in real assembly lines because a sudden detachment of one of these sensors could cause either a stop in the production line, or a defect in manufactured products. Lubricant or wear debris analysis is also commonly used for industrial robot joint health assessment. It consist on analysing the wear particles inside the oil that lubricates the joints. As illustrated in [17], any mechanical element working in contact with another mechanical element will deteriorate and degrade regardless of the design. A disadvantage of analysing wear debris in the lubricant is that it needs advanced laboratory equipment and it is highly time consuming. In addition, this method also needs the robot to be completely stationary [18].

According to the author's knowledge, there is only one article that suggests using torque data of industrial robot joints to assess their health status. Bittencourt et al. studied in [12] the feasibility of using torque data for industrial robot and repetitive machinery condition monitoring. However, they did not measure the torque with sensors. Instead, they calculated the torque by estimating it from the electric current. The electric current in the motors is directly proportional to the torque required by each joint. The higher the torque, the more electric current each joint will require. In their study, Bittencourt et al. used kernel density estimates and the Kullback-Leibler distance to detect deviations in the repetitivity of an industrial robot joint's torque [12]. They considered both real data from accelerated wear tests and simulated data. Industrial robots are presently manufactured with a torque sensor installed in each joint and therefore, no additional torque sensor needs to be installed. Moreover, torque data is also useful to monitor and control the energy consumption of the robots. A deteriorated robot joint should require higher torque to accomplish a specific task compared to a healthy robot joint. However, the feasibility of torque sensors to detect medium and long-term mechanical deterioration in industrial robot joints has not been proven and it remains unclear.

The novelty of the paper resides in three main contributions. First, we show the effectiveness of joint torque monitoring to detect motor brake failures inside robot joints. We perform an in depth mechanical inspection to find the root cause of a frequent failure of high payload industrial robots. Second, we emphasize the influence of the standby pose of industrial robots in the reduction of their RUL by analysing a dataset with more than 600 robots. Last but not least, we present and validate a methodology for industrial robot health assessment using torque sensors. The proposed methodology is based on the conclusions extracted from the experiments and the mechanical inspection carried out. The methodology proposed in this paper is applicable to any kind of 6 Degree-of-freedom (DOF) robot with any kind of load. The data is acquired in a non-intrusive way, as torque sensors are located inside the structure of the manipulator.

The manuscript is structured as follows: Section 2 describes the experiment carried out, as well as the obtained results. In Section 3 we perform an in depth root cause analysis of the mechanical fault detected in the experiment. Section 4 analyses a possible cause of the reduction of the remaining useful life of the robots and suggests preventive measures to enlarge their RUL. In Section 5 we propose

a methodology to monitor the health status of industrial robots based on the experiments explained in previous sections, and finally Section 6 sums up the main conclusions and future lines.

2. Experimental Design and Implementation

We designed an experiment to compare the torque applied by a faulty robot joint and a healthy one. If the mechanical wear has a significant effect in the effort of the joint, our hypothesis is that the faulty joint would require higher torque than a healthy joint to execute a given trajectory. Therefore, the methods selected to identify a faulty joint should focus on measuring the increment of the torque applied in the robot joints, whether they are statistical methods or machine learning models. Figure 1 describes the process of the experimental procedure carried out. First, a faulty robot wrist was removed from an automotive assembly line after years of uninterrupted work. The faulty robot caused a sudden stop in the production line and it was replaced by a new one. The experiment was performed using a 6 DOF industrial robot (ABB IRB 6400r), two robot wrists (the faulty wrist and the new one), two loads representing the 15% and 90% of the maximum payload of the robot and four torque sensors, two sensors for each wrist, located in the 5th and 6th joints. These sensors are factory built-in torque sensors and the robotic systems uses them in the control feedback-loop. The ABB IRB 6400r is a widely used industrial robot in the automotive industry with a maximum payload of 200 Kg.
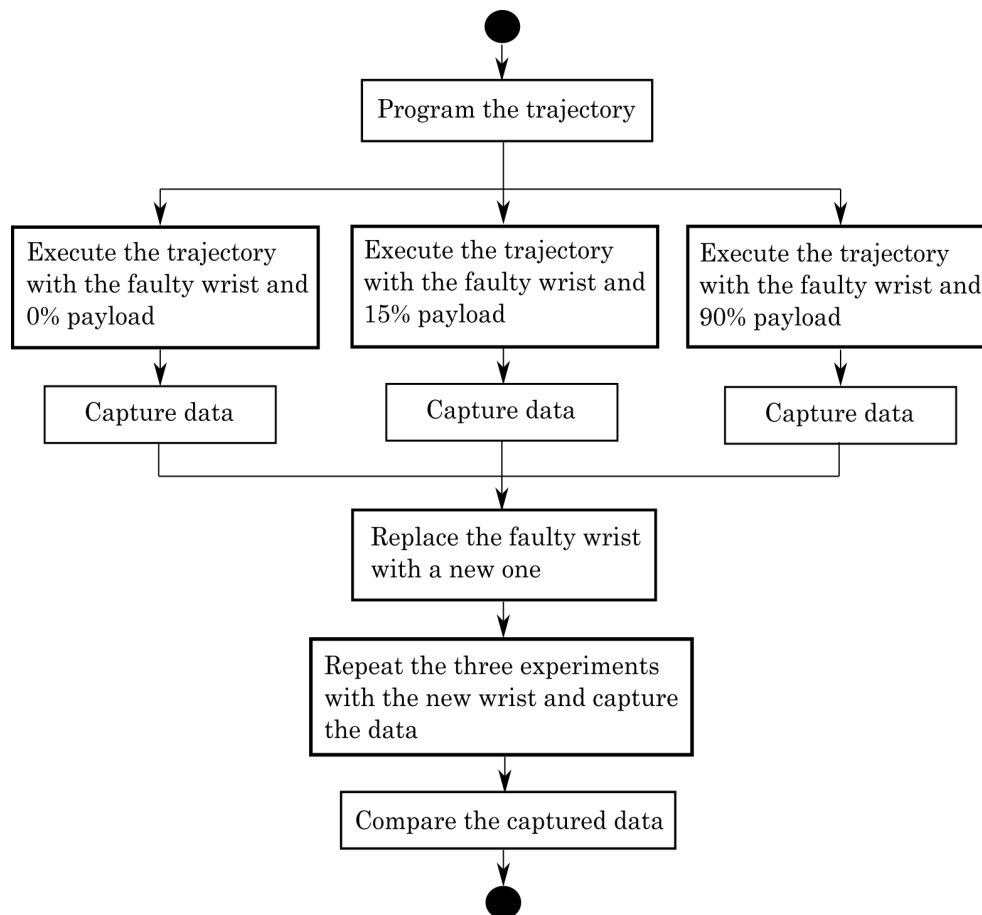

Figure 1. Flowchart of the experimental procedure carried out.

A non-trivial fixed trajectory was programmed in order to excite the robot joints. First of all, the faulty wrist was installed in the ABB robot in a laboratory facility, out of the production line. Then, the programmed trajectory was executed three times with three different loads each time. The loads represented the 0%, 15% and 90% of the maximum payload of the robot. We executed the trajectories and collected the torque data with a sampling rate of 100 ms. Afterwards, the faulty wrist

was removed and the new one installed in the same ABB robot. The trajectory was repeated again three times with the same three different loads in each repetition. Therefore we collected the data of the torque applied in the 5th and 6th joints throughout the six trajectory executions (three with the faulty wrist and tree with the new wrist).

After completing all these trajectories, torque signals were acquired and stored in csv files following the format specified in Table 1. The signals were stored as floating point numbers and using the standard unit (Nm) for the torque. We used the TCP/IP communication protocol to connect with the robot controller and capture the torque signals, which is an Industry 4.0 communication standard. The TCP/IP protocol is suitable for Industry 4.0 and Big Data scenarios, as it is able to interconnect large number of devices [19]. Some researchers have used the OPC-UA communication protocol [9] which is built on top of TCP/IP for data acquisition in industrial scenarios. The data shown in Figures 2 and 3 disclose an evident increment in the torque of the faulty wrist's 5th joint. This increment is clearly appreciable in all the three experiments and throughout the execution of the whole trajectory, therefore the effort required by the motor of the 5th joint was higher than expected with any of the three loads and in any robot pose or movement. In contrast, the torque of the 6th joint does not change significantly in any experiment.

Table 1. Example of the torque data captured by one robot in one experiment e.g., The column name *Torque_joint_5_A* refers to the torque acquired in the 5th joint of robot *A* (faulty robot).

Observation	Time (s)	Torque_Joint_5_A (Nm)	Torque_Joint_6_A (Nm)
1	0	0.819	−1.045
2	0.100	4.08	2.109
3	0.200	9.007	4.323
4	0.300	10.118	6.137
…	…	…	…

The increment in the torque is measured by first calculating the absolute value of the acquired signals. The absolute value of the torque in each joint is then integrated to calculate the total amount of torque applied throughout the whole trajectory in all the experiments. Once the total applied torque is calculated, the percentage of increase between the two wrists is calculated. Tables 2 and 3 show the results of the 5th and 6th joints respectively.

Table 2. Total torque of the 5th joint of the new and faulty wrists. *Load 1*, *Load 2* and *Load 3* represent the 0%, 15% and 90% of the maximum payload respectively.

	New (Nm)	Faulty (Nm)	Increase
Load 1	19,567	42,830	118.88%
Load 2	21,224	46,451	118.86%
Load 3	62,235	124,703	100.37%

Table 3. Total torque of the 6th joint of the new and faulty wrists. *Load 1*, *Load 2* and *Load 3* represent the 0%, 15% and 90% of the maximum payload respectively.

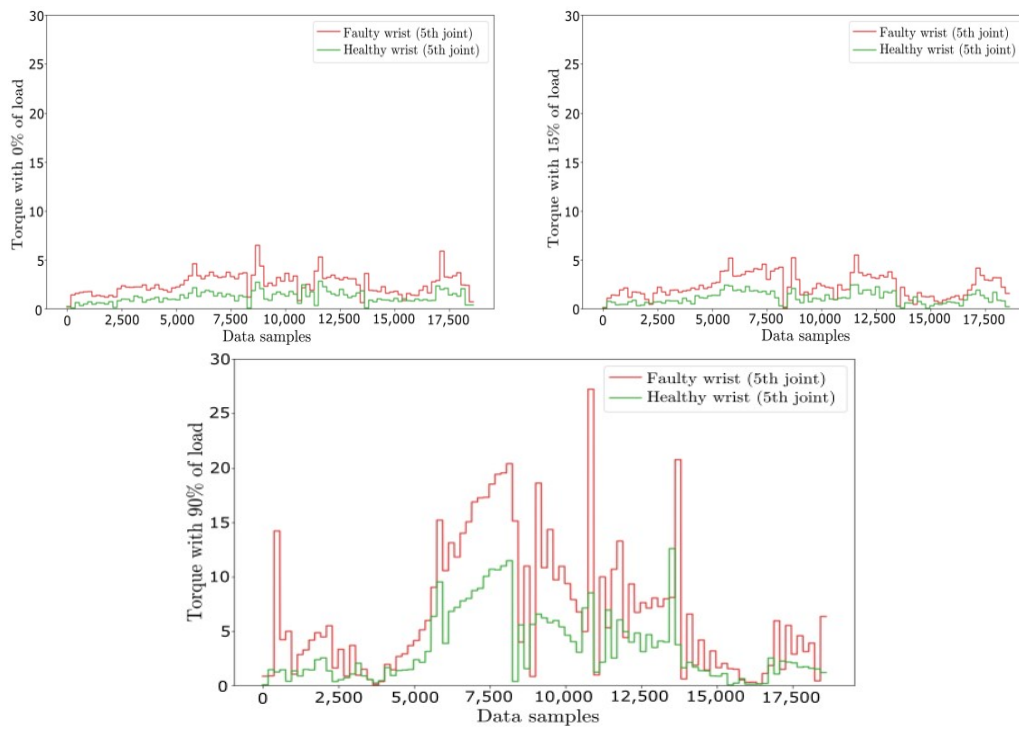|	New (Nm)	Faulty (Nm)	Increase
Load 1	17,910	19,039	6.31%
Load 2	20,852	19,982	−4.17%
Load 3	28,671	28,970	1.04%

Figure 2. Torque values of the 5th joint in a faulty wrist and in a healthy wrist with different loads and same trajectory.
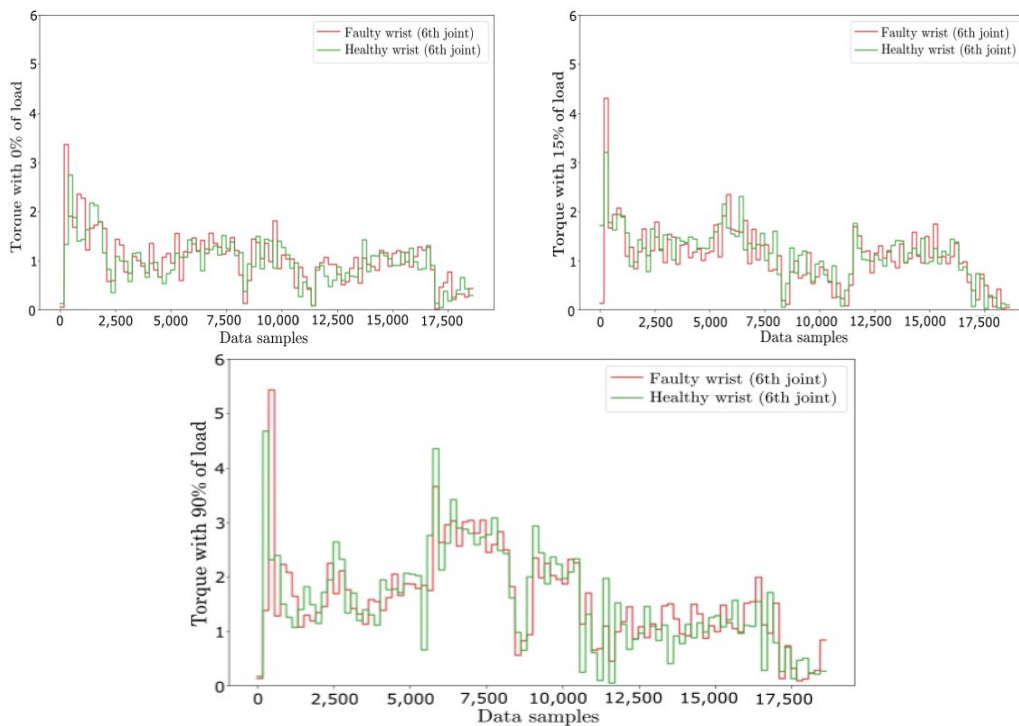

Figure 3. Torque values of the 6th joint in a faulty wrist and in a healthy wrist with different loads and same trajectory.

The increment in the torque is homogeneous, i.e., The torque increases in the whole trajectory and not only in certain movements or positions. The fact that the torque increases in the whole trajectory and not only in certain poses, reveals that the deterioration affects to the entire movement of the joint. The results also show that at the time of the failure, the electric consumption of joint 5 in the faulty wrist was at least twice as high as expected for a healthy joint.

Although the acquired data effectively detects the wear in the joint, the detected increment is not enough on its own to deduce a root cause of the fault. Thence, we conducted a root cause analysis with an in-depth mechanical inspection in order to identify the cause.

3. Root Cause Analysis of the Faulty Joint

3.1. Mechanical Inspection

The first step of the mechanical inspection consisted on disassembling the faulty wrist. The 5th joint of the wrist is composed of an electric motor and a speed reducer. First, we inspected the gears of the speed reducer, shown in Figure 4. We did not find any evidence of wear or pitting in the surface of the gears and there was no apparent damage in the gears that could cause the significant increment detected in the torque. The lubricant oil of the reducer was extracted and analysed in the process of disassembling the faulty wrist. We confirmed that the lubricant was within the quality tolerance limits as no metallic debris was found in the oil.
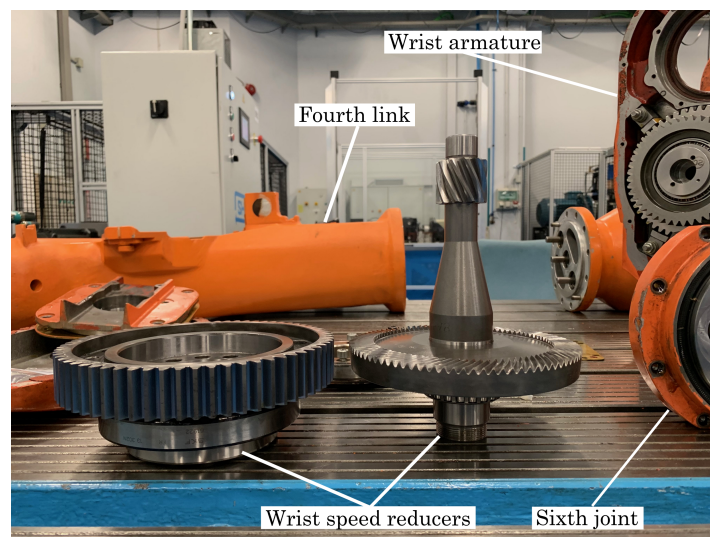

Figure 4. Mechanical inspection of the gears, bearings and motors of the wrist.

Afterwards, we examined the motor of the 5th joint. An increment such as the one detected in the experiment could be caused due to a significant decrease in the motor's coil resistance. We measured the resistance of the coil using an ohmmeter and compared it with the resistance of the coil of a new motor. The resistance values in both coils were identical. Hence, the motor's coil was dismissed as the cause of the joint fault.

3.2. Analysis of the Motor Brake

After analysing the condition of the speed reducer and the motor, we inspected the brake of the motor. The brake of the 5th joint is a permanent magnet brake that stops the motor when the robot is shut down or when an emergency stop is required. As illustrated in the schematic of Figure 5 this kind of brakes have three main parts: a metallic armature, a field coil and a neodymium (NdFeB) permanent magnet. The brake works in the following way: when the robot shuts down or makes an emergency stop, there is no voltage applied to the coil and the permanent magnet attracts the armature, stopping the rotation of the motor. In contrast, if the robot controller applies 24V to the field coil of the brake, it produces a magnetic field compensating the magnetic field created by the permanent magnet and the motor is released.
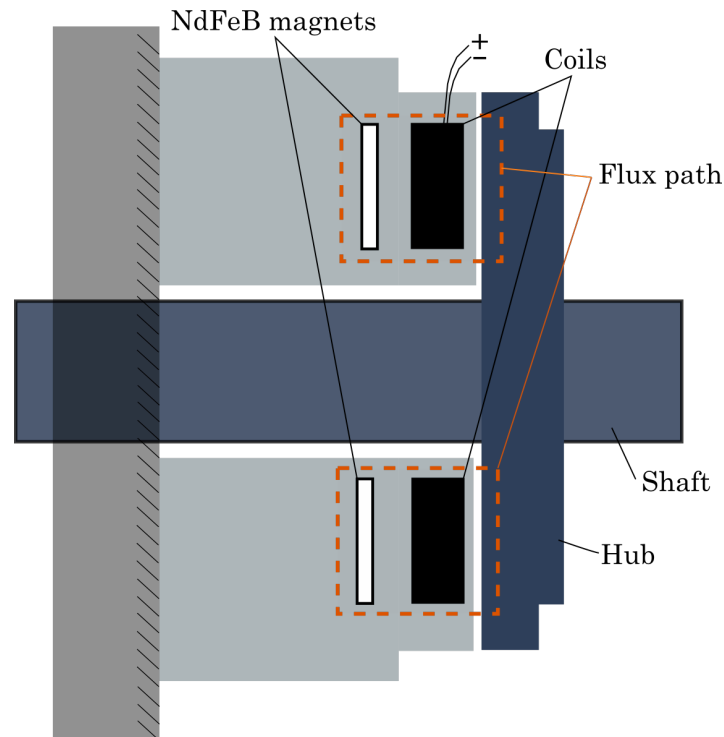
Figure 5. Schematic of the motor brake.

We measured the resistance of the brake's coil and compared it with the resistance of a completely new coil. In both cases the values reached $15.4\,\Omega$. Therefore, the coil of the brake could not be the cause of the detected torque increment.

Finally, we inspected the permanent magnets of the brake. The permanent magnets used in this brake are squared NdFeB magnets. We noticed a slight deformation in the corners of the magnets, as some magnetic particles were detached from them. We found the particles filling the space where the magnets are located. Figure 6 shows the permanent magnets inside the brake of the faulty joint compared to a completely new brake. In addition, Figure 6 shows that the colouring of the brake's armature was changed. These kind of stainless steel armatures, have a metallic light silver colour when manufactured. However, the inspected brake had a reddish coloring as a consequence of oxidation.
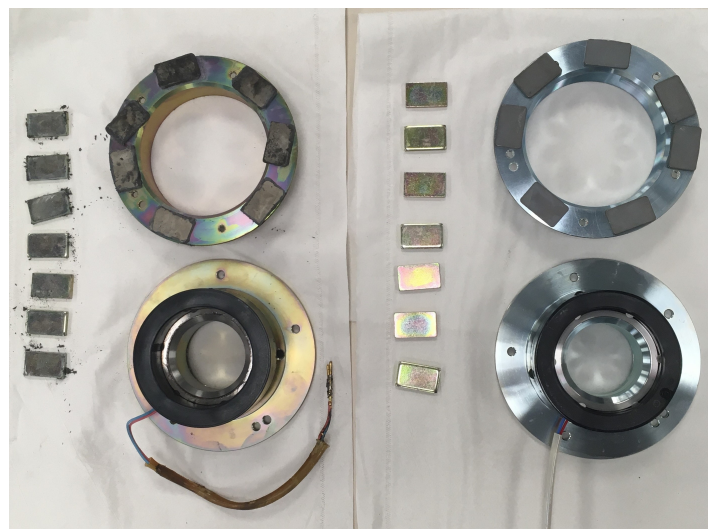

Figure 6. The motor brake of the faulty joint and its permanent magnets (**left**) compared to a completely new motor brake (**right**).

We performed two tests to diagnose the health status of the permanent magnets. The first test consisted on measuring the M(H) hysteresis curve of the magnets. Then, we magnetized the permanent magnets and measured again the M(H) hysteresis curve after the magnetization. The results of the tests are shown in Figure 7.
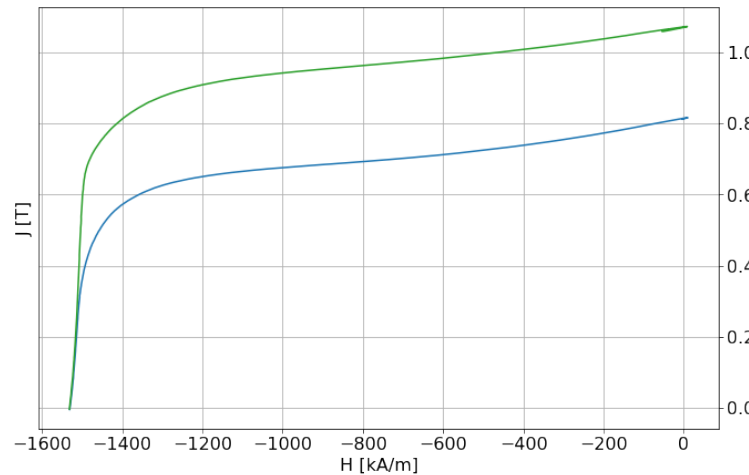

Figure 7. Magnetic hysteresis curve of the motor brake's permanent magnet before (blue) and after (green) magnetization.

There is a 24% loss from 0.814 T before magnetization to 1.071 T after the magnetization. This significant magnetic field loss has a direct impact in the malfunction of the motor's brake. As a consequence, the brake constantly resists the movement of the motor. This produces the torque increment in the 5th joint throughout the whole trajectory identified in Section 2.

The second test consisted on measuring the magnetic hysteresis curve at different temperatures. Figure 8 shows the different M (H) curves at 26, 80, 100 and 120 °C and Table 4 shows the magnetic properties of the permanent magnet at these temperature regimes. Br (T) is the residual induction or flux density, that is the magnetic induction corresponding to zero magnetizing force in a magnetic material after saturation. Hci (kA/m) is the intrinsic coercive force of a material and indicates its resistance to demagnetization.
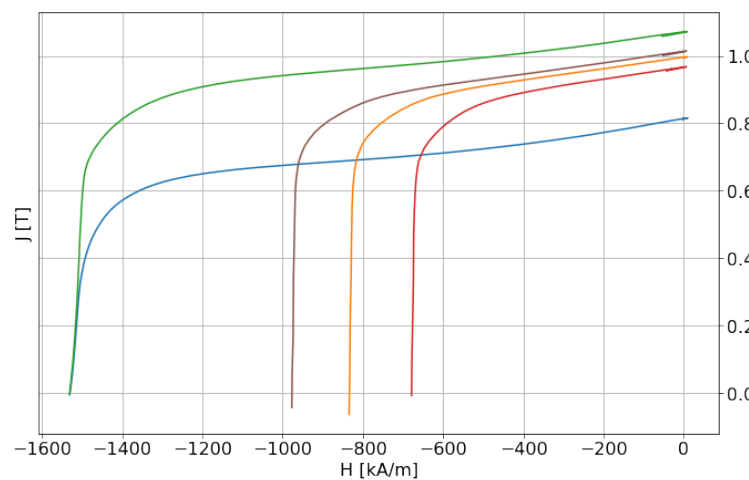

Figure 8. Magnetic hysteresis curve of the permanent magnet at 26 (green), 80 (brown), 100 (orange) and 120 °C (red).

Table 4. Magnetic properties of the permanent magnet at the measured temperatures.

T (°C)	Br (T)	Hci (kA/m)
26	1.071	1531
80	1.013	976.9
100	0.9957	833.4
120	0.9668	678.5

There are two additional considerations that have to be taken into account. The technical specifications of the 5th joint's motor indicates that the surface temperature of the motor can reach up to 140 °C. Therefore, the temperatures inside the motor brake could be even higher than the temperatures reached in the test. Moreover, in the recently published work by M. Haavisto [20] the time dependent demagnetization of NdFeB permanent magnets is extensively investigated. She experimentally proved that this type of magnets can be demagnetized if exposed to higher than 80 °C for a long period of time. This conclusion is especially relevant for industrial robots working in assembly lines for years uninterruptedly.

These results of the tests, the mechanical inspection carried out, the state of the motor brake, as well as the previously mentioned PhD dissertation [20], give us enough evidence to conclude that the temperatures inside the motor of the 5th joint of the robot, reached high enough temperatures for sufficient time to produce a magnetization loss in the permanent magnets of the motor brake. This caused the failure in the wrist and the increased torque values shown in Section 2.

4. The Influence of the Standby Pose in Robot Failures

In real automotive manufacturing production lines, there is substantial difference in the waiting and working time of the robots depending on their process and location. Some of them execute trajectories almost uninterruptedly, while others spend most of the time waiting. The most active robots work approximately 85% of the total operative time and the most inactive robots only around 20%.

In the previous section, we identified the root cause of the wrist failure in the demagnetization of the motor magnets. This demagnetisation, as well as the oxidation of the brake, is produced by a relatively high temperature prolonged over long periods of time. In this section, we analyse two factors that strongly influence the overheating in industrial robot wrists: the pose in which the robots wait for the next product and the load they carry.

We collected a dataset with more than 600 robots of a real manufacturing assembly line to analyze the influence of the load and the waiting pose in robot wrist failures. The information stored in the dataset was structured in three columns: the mechanical failures of the 5th joint in the last 15 years (57 failures in total), the load of the robots and the orientation of their 5th joint. The orientation of the 5th joint represents the verticality of the joint. As illustrated in Figure 9 if the joint is completely vertical to the ground, the orientation will have a value of 0 and if the joint is completely horizontal to the ground, the value of the orientation will be 90. Therefore, when we talk about the orientation, we are refering to the verticality of the 5th joint when the robot waits stationary for the next product.
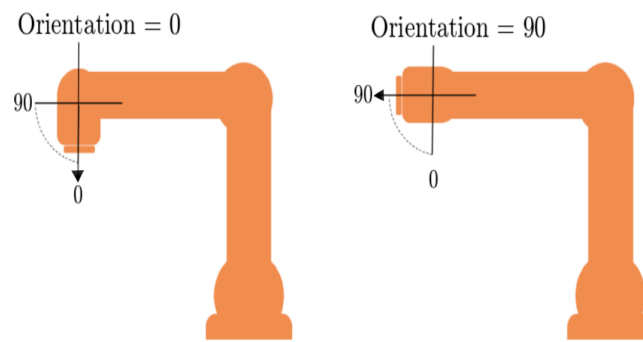
Figure 9. Orientation value in the dataset represents the *verticality* or *horizontality* of the 5th joint.

Figures 10 and 11 show the difference in distribution in the load and standby orientation of the 5th joint of more than 600 industrial robots. The boxplots are grouped by robots that never had a mechanical failure in that joint (0) and robots that did fail (1). These boxplots show that robots that had a failure in the 5th joint tend to work with higher loads and hold the load in a more horizontal pose. The differences in the load and orientation are shown in Table 5. There is a difference of 29.71 Kg in the mean of the load between the robots that have failed and the robots that have not failed yet. The mean of the standby orientation of the 5th joint is 9.17 ° closer to the parallel of the ground for robots that have failed.

These results show that both the carried load and the orientation of the 5th joint while waiting have a significant impact in the RUL of industrial robot wrists. The fifth joint of the robot requires more effort to hold a heavier load and to hold a given load in a more horizontal orientation. Thus, this effort results in a higher torque that the motor must apply, which increases the current in the motor coil and the temperature of the motor.

Table 5. Standby orientation and load means with recorded historical failures and without failures.

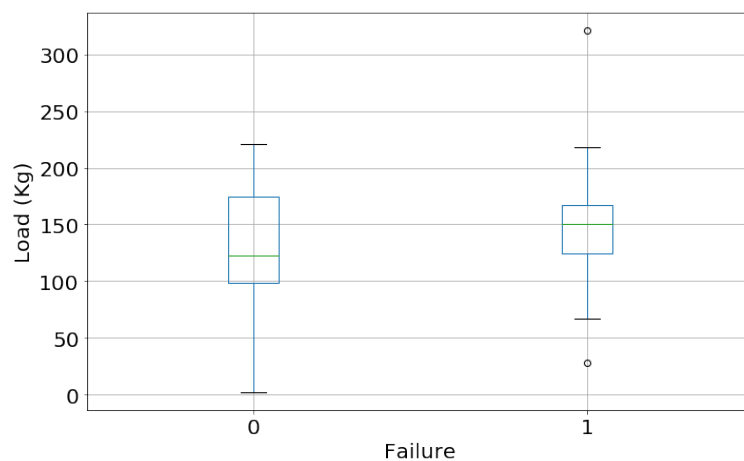|	Orientation (°)	Load (Kg)
With failure	71.39	148.5
Without failure	62.22	118.79

Figure 10. Mean load of robots without recorded failures (0) and with failures (1).
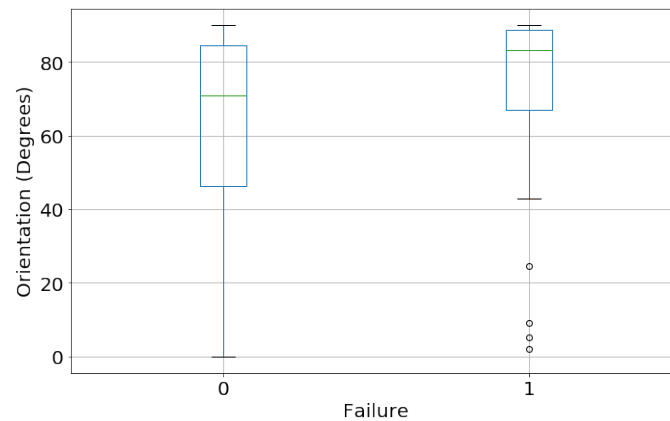
Figure 11. Mean standby orientation no recorded failures (0) and with failures (1).

5. The Health Assessment Program Methodology

Based on the results of the previous sections, we propose a methodology for diagnosing the health status of industrial robot joints with torque signature analysis. The diagram representing the methodology can be seen in Figure 12. The main idea behind the proposed methodology is that a joint that suffers a mechanical degradation will require higher torque to execute a certain trajectory than a healthy one. As the time goes by, the mechanical elements attached to the motor (i.e., The brake and the reducer) will inevitably suffer mechanical deterioration. This will require higher effort to execute the same trajectory. To illustrate the methodology, let's say that a robot R_1 executes a certain program P_1 and needs to apply torque T_1 in a joint to complete the trajectory. If there is any mechanical deterioration, the system will be less efficient, but the robot controller will make sure that this deterioration does not affect the accuracy of the robot. Even if the accuracy remains invariant, to finish the same program P_1 the required torque now (T_2) will be higher than before ($T_2 > T_1$).

5. Whenever a new data acquisition is required, the process is repeated and new torque signals are acquired to compare them with the previously stored values.

1. A specific tool-trajectory configuration is defined for a given robot.

2. The trajectory is executed in the robot with the previously defined configuration.

3. Torque data is captured while the robot executes the trajectory.

4. The acquired torque data is stored in a server as a reference along with the robot's ID.

6. Finally, torque data from previous captures is compared with recent acquisitions to evaluate the possible deterioration.
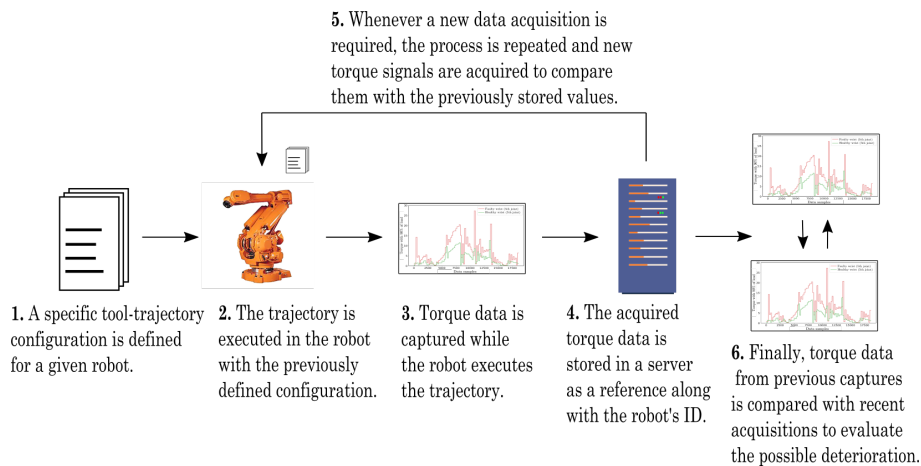
Figure 12. Diagram of the proposed methodology. First, the trajectory and tool are defined. Then, the program is executed and torque data is acquired. The recorded data is stored in a server as a reference along with the robot's ID. The process is periodically repeated and the new signals are compared with previously recorded ones to diagnose a possible deterioration.

We therefore propose to use a specific trajectory-tool combination in the robots of the production line to assess their current health status. As described in the diagram of Figure 12 robots will execute a predefined non-trivial trajectory with a known load and they will require a certain amount of torque in each joint to complete this trajectory. To acquire torque data in all the joints, the trajectory must use the whole set of joints comprising the robot manipulator. We will call *Health Assessment Program* (*HAP*) to that predefined trajectory-load combination. These two specifications will always have to

remain unchanged in order to make a fair comparison of the results. However, an advantage of the methodology is that the precise shape, center of mass and inertia of the load are not required to be known or modeled.

The first step is to execute the trajectory with the robot attaching the corresponding load. The torque of each joint will be recorded during the the whole process, producing a digital *signature* of the torque of each joint. This initial torque data or *signature* will be used as a reference for that particular robot. This initial data will be stored with an identification number of the robot. Whenever we want to analyse the mechanical deterioration of the joints of that robot, we will run the *HAP* again and compare the previously stored values with the recently acquired ones. If there is no change in the torque values, we can conclude that there is no significant mechanical deterioration in the joints yet. In contrast, if there is some increase in the torque of a certain joint, it will mean that the motor of that joint is requiring more effort than expected.

The proposed methodology is applicable to any joint or industrial robot. In addition programming the *HAP* as an additional trajectory to the usual routine of the robots is enough. It is not necessary to take the robot off the production line to diagnose it. Which is a significant advantage compared to existing condition monitoring techniques.

6. Discussion and Conclusions

We reported a methodology for industrial robot health assessment. The methodology was validated experimentally comparing the torque of two robot wrists. These results show that torque sensors provide reliable information to detect mechanical deterioration of an industrial robot's joint. We carried out the comparisons with different loads and the increment in the torque was clearly appreciable with the three tested loads. Therefore, the methodology is proved to be useful with any load configuration. The recorded torque data shows an homogeneous increase in the faulty wrist. The source of the malfunction was located in the permanent magnets of the motor brakes with an in depth mechanical inspection. We measured the magnetic field of the permanent magnets and the hysteresis curves showed a 24% of magnetic field loss in the permanent magnets of the faulty joint. The effect of this magnetic field loss can be effectively detected with the proposed methodology.

A direct conclusion of the work is that the electrical consumption of the faulty joint was approximately twice that of a healthy joint. Therefore, even if a robot does not show any apparent malfunction it might still be working in conditions which are far from ideal due to mechanical deterioration and fatigue. The proposed method could help manufacturers to monitor not only the mechanical condition of the robot joints but also the electrical over-consumption i.e., Detecting the most energy-consuming robots or work cells. Controlling the energy consumption of robots is a fundamental factor to achieve sustainable factories and to reduce pollution.

Another significant advantage of the methodology is that torque measurement is done inside the robot's physical structure. As we mentioned in the introduction, if a sensor or a wire installed in the outside part of the robot's structure detaches and falls into the production line, it could cause significant damage to the product being manufactured or even stop the production line. Therefore, since torque sensors are inside the robot's physical structure, this possible inconvenience is dismissed. Last but not least, the methodology is applicable to any industrial robot, as long as the acquired data is compared with robots of the same model. Hence, our approach does not depend on the robot manufacturer or the robot type. It only depends on the programmed trajectory and the carried load, which are both configurable by researchers and practitioners.

A limitation of the presented work is that the detection of torque deviation depends on a pre-defined tool and trajectory configuration. Therefore, if either of these two characteristics change, torque signals would also inevitably change and the data regarding the monitored robot should be readjusted. Another limitation of the presented work is that the execution of the *Health Assessment Program* requires the robot to momentarily stop its normal production behavior to execute a pre-defined trajectory and acquire the correct torque signals.

An identified future line of work is to implement machine-learning models to detect anomalies in the torque of robot joints with different tool and trajectory configurations. Although our approach requires a specific trajectory and tool configuration for the data to be comparable, a machine-learning model might be flexible enough to detect deviations with different trajectory and tool configurations and extrapolate the behavior learned in one use case to the rest. Another interesting future line of work would be to use the proposed methodology to train predictive models to estimate the RUL of industrial robots in real production line conditions. Our methodology effectively detects deviations from the normal behavior of robot joints in real world scenarios, but further research is needed to accurately assess the RUL of the monitored robotic systems. Finally, torque data monitoring could also be used to find an optimal standby pose of industrial robots in order to minimize the effort of the joints. Based on the observed influence of the waiting pose in the wrist failures (Section 4). An optimal standby pose for a given robot model and tool, could minimize the effort and thus torque and temperature of the joints, increasing their RUL and optimizing the energy consumption.

Author Contributions: Conceptualization, U.I., I.A. and U.Z.; methodology, U.I. and I.A.; software, U.I. and A.E.; validation, I.A., A.E. and U.Z.; formal analysis, U.I. and A.E.; investigation, U.I.; resources, I.A. and U.Z.; data curation, U.I.; writing—original draft preparation, U.I.; writing—review and editing, U.I., I.A. and U.Z.; visualization, U.I. and A.E.; supervision, I.A. and U.Z.; project administration, I.A. and U.Z.; funding acquisition, I.A. and U.Z. All authors have read and agreed to the published version of the manuscript.

Conflicts of Interest: The authors declare no conflict of interest. The funders had no role in the design of the study; in the collection, analyses, or interpretation of data; in the writing of the manuscript, or in the decision to publish the results.

References

1. Qiao, G.; Weiss, B.A. Advancing measurement science to assess monitoring, diagnostics, and prognostics for manufacturing robotics. *Int. J. Progn. Health Manag.* **2016**, *7*. [CrossRef]
2. Jaber, A.A. *Design of an Intelligent Embedded System for Condition Monitoring of an Industrial Robot*; Springer: Berlin/Heidelberg, Germany, 2016.
3. Peng, Y.; Dong, M.; Zuo, M.J. Current status of machine prognostics in condition-based maintenance: A review. *Int. J. Adv. Manuf. Technol.* **2010**, *50*, 297–313. [CrossRef]
4. Qin, Y. A new family of model-based impulsive wavelets and their sparse representation for rolling bearing fault diagnosis. *IEEE Trans. Ind. Electron.* **2017**, *65*, 2716–2726. [CrossRef]
5. Blancke, O.; Tahan, A.; Komljenovic, D.; Amyot, N.; Hudon, C.; Lévesque, M. A hydrogenerator model-based failure detection framework to support asset management. In Proceedings of the 2016 IEEE International Conference on Prognostics and Health Management (ICPHM), Ottawa, ON, Canada, 20–22 June 2016; pp. 1–6.
6. Dalla Vedova, M.D.; Germanà, A.; Berri, P.C.; Maggiore, P. Model-Based Fault Detection and Identification for Prognostics of Electromechanical Actuators Using Genetic Algorithms. *Aerospace* **2019**, *6*, 94. [CrossRef]
7. Bittencourt, A.C. Modeling and Diagnosis of Friction and Wear in Industrial Robots. Ph.D. Thesis, Linköping University Electronic Press, Linköping, Sweden, 2014.
8. Tao, F.; Qi, Q.; Liu, A.; Kusiak, A. Data-driven smart manufacturing. *J. Manuf. Syst.* **2018**, *48*, 157–169. [CrossRef]
9. Mourtzis, D.; Vlachou, E.; Milas, N. Industrial Big Data as a result of IoT adoption in manufacturing. *Procedia CIRP* **2016**, *55*, 290–295. [CrossRef]
10. Sun, X.; Jia, X. A fault diagnosis method of industrial robot rolling bearing based on data driven and random intuitive fuzzy decision. *IEEE Access* **2019**, *7*, 148764–148770. [CrossRef]
11. Borgi, T.; Hidri, A.; Neef, B.; Naceur, M.S. Data analytics for predictive maintenance of industrial robots. In Proceedings of the 2017 International Conference on Advanced Systems and Electric Technologies (IC_ASET), Hammamet, Tunisia, 14–17 January 2017; pp. 412–417.

12. Bittencourt, A.C.; Saarinen, K.; Sander-Tavallaey, S.; Gunnarsson, S.; Norrlöf, M. A data-driven approach to diagnostics of repetitive processes in the distribution domain—Applications to gearbox diagnostics in industrial robots and rotating machines. *Mechatronics* **2014**, *24*, 1032–1041. [CrossRef]

13. Vallachira, S.; Orkisz, M.; Norrlöf, M.; Butail, S. Data-driven gearbox failure detection in industrial robots. *IEEE Trans. Ind. Inform.* **2019**, *16*, 193–201. [CrossRef]

14. Mourtzis, D.; Milas, N.; Athinaios, N. Towards machine shop 4.0: a general machine model for CNC machine-tools through OPC-UA. *Procedia CIRP* **2018**, *78*, 301–306. [CrossRef]

15. Vogl, G.W.; Calamari, M.; Ye, S.; Donmez, M.A. A sensor-based method for diagnostics of geometric performance of machine tool linear axes. *Procedia Manuf.* **2016**, *5*, 621–633. [CrossRef]

16. Liu, X.; Wu, X.; Liu, C.; Liu, T. Research on condition monitoring of speed reducer of industrial robot with acoustic emission. *Trans. Can. Soc. Mech. Eng.* **2016**, *40*, 1041–1049. [CrossRef]

17. Bhushan, B. *Introduction to Tribology*; John Wiley & Sons: Hoboken, NJ, USA, 2013.

18. Ebersbach, S.; Peng, Z.; Kessissoglou, N. The investigation of the condition and faults of a spur gearbox using vibration and wear debris analysis techniques. *Wear* **2006**, *260*, 16–24. [CrossRef]

19. Wang, L.; Wang, G. Big data in cyber-physical systems, digital manufacturing and industry 4.0. *Int. J. Eng. Manuf. (IJEM)* **2016**, *6*, 1–8.

20. Haavisto, M. Studies on the Time-Dependent Demagnetization of Sintered NdFeB Permanent Magnets. 2013. Available online: https://trepo.tuni.fi/handle/10024/115203 (accessed on 13 April 2020).

Publisher's Note: MDPI stays neutral with regard to jurisdictional claims in published maps and institutional affiliations.